Supporting Information

Efficient NiO*x* Hole Transporting Layer obtained by the oxidation of Metal Nickel Film for Perovskite Solar Cells

Shangzheng Pang, Chunfu Zhang*, Hang Dong, Dazheng Chen, Weidong Zhu, He Xi, Jingjing Chang, Zhenhua Lin, Jincheng Zhang, and Yue Hao

Wide Bandgap Semiconductor Technology Disciplines State Key Laboratory, Shaanxi Joint Key Laboratory of Graphene, School of Microelectronics, Xidian University, Xi'an 710071, China

*Corresponding author: cfzhang@xidian.edu.cn

Experimental section

Materials

Methylammonium iodide (CH_3NH_3I, 99.8%) and Formamidinium iodide ($HC(NH_2)_2I$, 99.8%) were acquired from Dyesol. Lead (II) iodide (PbI_2, 99.999%), Lead (II) chloride ($PbCl_2$, 99.999%), and Bathocuproine (BCP, 96%) were purchased from Alfa. Phenyl-C61-butyric acid methyl ester ($PC_{61}BM$, 98%) was bought from nano-c. Poly(3,4-ethy-lenedioxythiophene):poly(styrenesulfonate) (PEDOT:PSS, Clevios PVP Al 4083) was bought from Heraeus. Nickel nitrate ($Ni(NO_3)_2 \cdot 6H_2O$), N,N'-Dimethylformamide (DMF, 99.8%), Chlorobenzene (anhydrous, 99.8%) and Isopropanol (IPA, 99.5%) were obtained from Sigma. All the materials were used as received without further purification.

Preparation for the NiO*x* thin film

For the solution-processed NiO*x*, 270.79 mg $Ni(NO_3)_2 \cdot 6H_2O$ (1.0 mmol) was dissolved in 2-methoxyethanol (10 ml). The solution was stirred at 50℃ for 1 h and then10 μl acetylacetone was added to the solution. The mixed solution was further stirred for overnight at the room temperature and ready for use. For the Ni-oxidized NiO*x*, Ni was evaporated on the FTO/Glass substrate and then ready for the following process.

Film formation and device fabrication

Planar inverted PSCs were fabricated on pre-patterned fluorine-doped tin oxide (FTO) glass substrates (around 2x2.5 cm^2 in size, 7 Ω per square). The patterned FTO glass substrates were sequentially ultrasonic cleaned with detergent, de-ionized water,

acetone, and isopropyl alcohol (IPA) at 50°C for 15 min, respectively. Then the FTO substrates were dried with nitrogen and treated in a UV ozone oven for 15 min. For the solution processed NiO*x*, a thin layer of NiO*x* was spin-coated on the substrates at 3000 rpm for 45 s and annealed at 250 °C for 1h. For Ni-oxidized NiO*x*, the Glass/FTO/Ni triple layers were annealed at 500℃ in air for 15min. Finally the substrate was cooled in the stink cupboard for 15min. For the devices based on the PEDOT:PSS HTL, PEDOT:PSS was spin-coated on the substrates at 7000 rpm for 40 s and annealed at 150°C for 15 min to act as a comparison. After that, the substrates were transferred into a nitrogen-filled glove box. For the one-step solution deposition method, the $FA_{0.3}MA_{0.7}PbI_{2.8}Cl_{0.2}$ precursor solution was prepared by mixing 1.26 M PbI_2, 0.14 M $PbCl_2$, 0.945 M MAI and 0.405 M FAI in the cosolvent of DMSO:GBL (3:7 v/v) and stirred for 1 h at 75 ºC. The solution was then spun coated onto the HTL layer with solvent engineering method. Briefly, the spin coating process was programmed to run at 1000 rpm for 20 s and then 4000 rpm for 40 s. When the spinning was at 40 s, 350 µl anhydrous chlorobenzene was injected onto the substrates. The perovskite films were solvent annealed on the hotplate at 100℃ for 35 min. For the two-step sequential deposition method, 0.85 M PbI_2 and 0.15 M $PbCl_2$ were dissolved in the solvent of DMF (named PbX_2 solution) and stirred for 2 h at 75 °C. 70 mg MAI and 30 mg FAI were dissolved in the solvent of IPA with 0.9 vol% DMF. Around 75 µl PbX_2 precursor, which was pre-heated to 75 °C, were spun to the NiO*x* covered FTO substrates. Briefly, the spin coating process was programmed to run at 3000 rpm for 45 s. Then MAI(FAI) was spin-coated on top of

the dried PbI_2 layer at 3000 rpm for 45 s. All of the films were thermally annealed on the hotplate at 100 °C for 10 min. Next, a layer of PCBM (20 mg/ml in chlorobenzene) was spin-coated on the top of the perovskite layer at 2000 rpm for 40s. After that, a thin layer of BCP (0.5 mg/ml in IPA) was spin-coated on the top of the PCBM layer. The devices were finished by thermally evaporated 100 nm Ag. All the devices had an effective area of 7 mm^2.

In this work metal Ni is firstly deposited on the FTO/glass substrate by E-beam evaporator and then converted to the NiO*x* by exposing it in the air with the help of annealing. The thickness of Ni is calculated based on the deposition rate, which in turn was determined with a in situ quartz crystal monitor. The accuracy of quartz crystal monitor is calibrated by the thickness measurement by step profiler (AMBIOS, XP-1). According to the 3D growth (Volmer–Weber growth) of Ni, the thickness given here had to be a nominal value obtained by the monitor, representing the amount of Ni on the sample. This thickness estimated method has been calibrated by cross sectional SEM and ellipsometry measurements [1], and used in previous research reports [1-2].

Oxidizing metals and forming metal oxides have been many reported in previous works. There are some corresponding relationships of the thickness between material and material oxides which characteristics have been used in SiO_2, Al_2O_3 and CuO growing[3-5]. It is feasible to control the thickness of Ni-oxidized NiO*x* by controlling that of metal Ni in our work.

Materials and device characterization

The morphology measurement of the perovskite layers was taken by scanning electron microscopy (SEM) (JSM-7800F). X-ray diffraction (XRD) test was conducted on Bruker D8 Advance XRD. The transmittance and absorption spectra of different samples were recorded with an UV-visible spectrophotometer (Perkin-Elmer Lambda 950). Photoluminescence spectra were collected on an Edinburgh Instruments FLS920 Spectro fluorometer, and the excitation wavelength was 633 nm. Photovoltaic performances were measured by using a Keithley 2400 source meter under simulated sunlight from XES-70S1 solar simulator matching the AM 1.5G standard with an intensity of 100 mW/cm^2. The system was calibrated against a NREL certified silicon reference solar cell. Incident photo-to-current conversion efficiencies (IPCEs) of PSCs were measured by the solar cell quantum efficiency measurement system (SCS10-X150, Zolix instrument. Co. Ltd). Steady photoluminescence was measured using the Pico Quant Fluotime 300 by using a 510 nm picosecond pulsed laser.

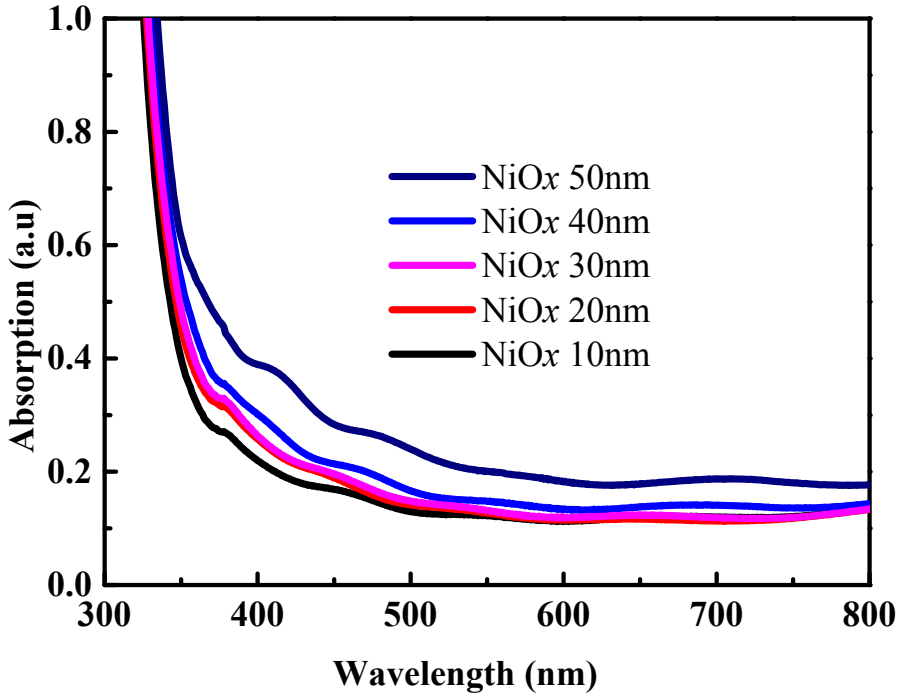

Fig. S1. Optical absorption of Glass/FTO/NiO*x* layer

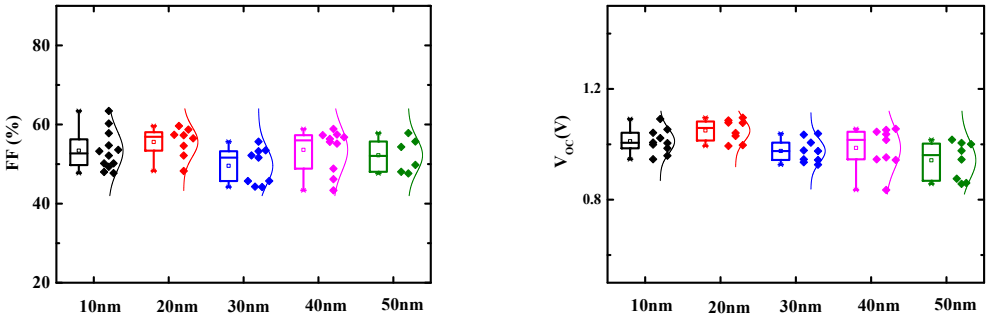

(a) (b)

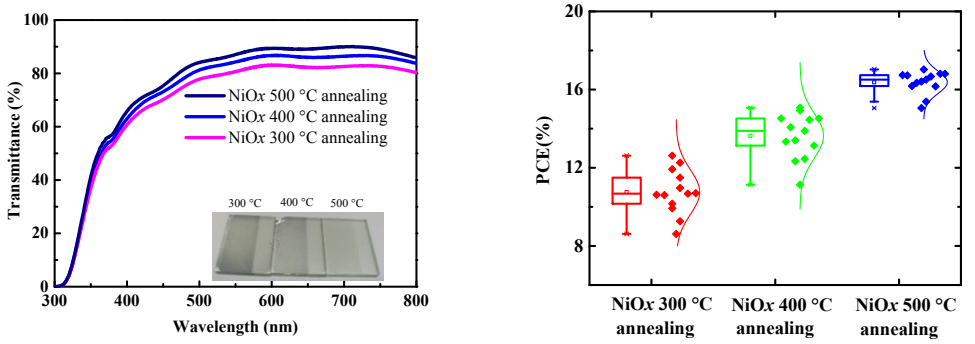

(c) (d)

Fig. S2. (a) Statistical results of fill factor and (b) statistical results of open circuit voltage for the perovskite devices based on the Ni oxidized NiO*x* HTLs. (c)Ni-oxidized NiO*x* layer with different annealing temperatures (d) PCE of PSCs based on Ni-oxidized NiO*x* layer with different annealing temperatures

Band gap calculation theory

The absorption coefficient α can be calculated as follows: $T = A\exp(-\alpha d)$, where T is the transmittance of the NiO*x* film, A is a constant and approximate unity, and d is the film thickness. The optical band gap of the NiO*x* films is determined by applying the Tauc model in the high absorbance region: $\alpha h\nu = D(h\nu - E_g)^n$, where $h\nu$ is the photon energy, E_g is the optical band gap, D is a constant, and n equals to 1/2. The direct optical band gap of the NiO*x* thin films was obtained by plotting $(\alpha h\nu)^{1/2}$ versus $h\nu$. Compared to solution processed NiO*x* with a band gap of 3.72 eV, the Ni oxidized NiO*x* exhibited slightly larger band gap of 3.83 eV.

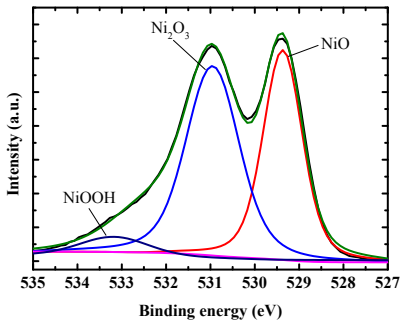

(a)

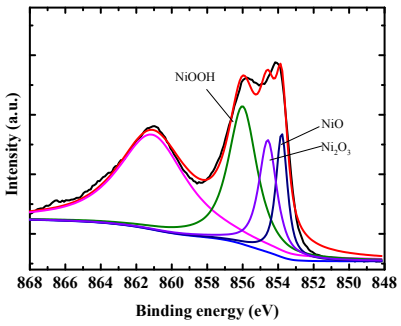

(b)

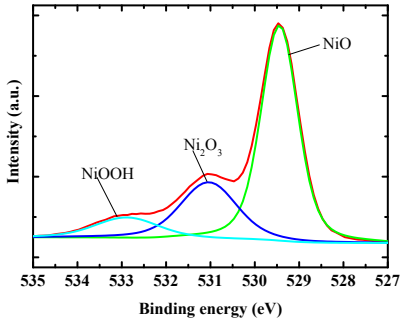

(c)

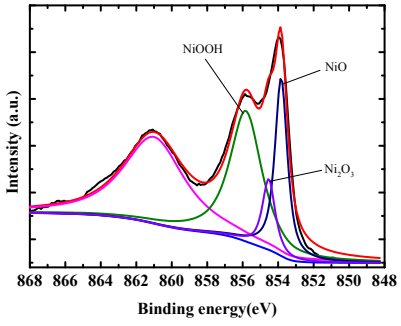

(d)

Fig. S3. XPS spectra of O1s (a,c) and Ni 2p (b,d) core level for solution processed (a-b) and Ni oxidized (c-d) NiO*x* thin films on FTO substrates.

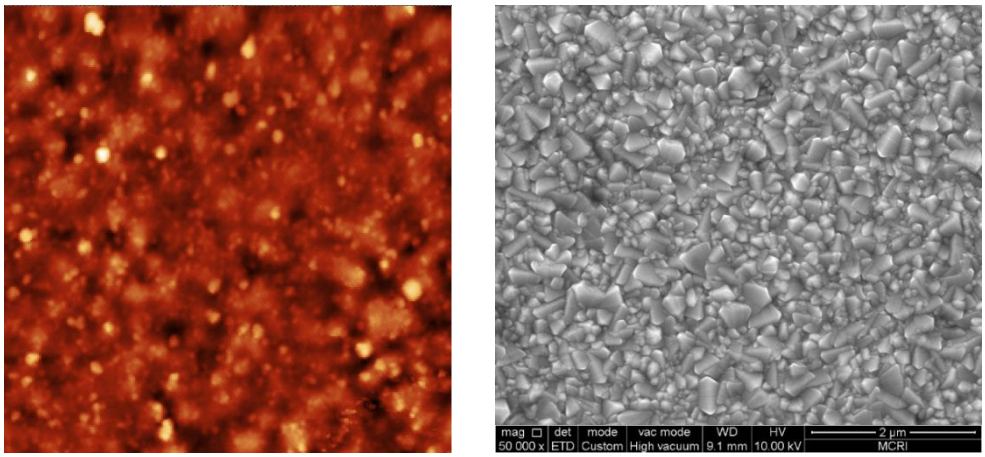

(a) (b)

Fig. S4. (a)AFM images of solution processed PEDOT:PSS (RMS=9.6nm) SEM of (b)solution processed PEDOT:PSS

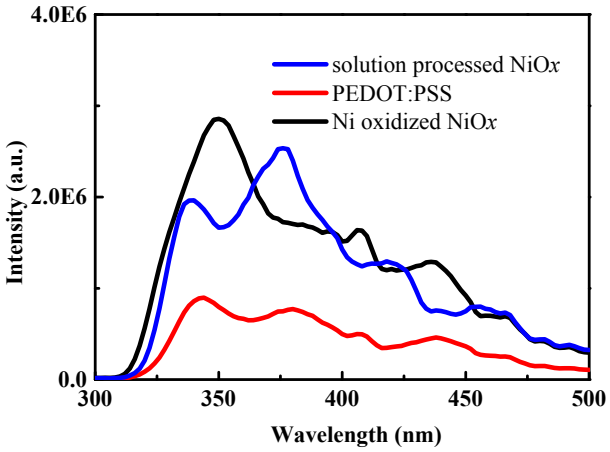

Fig. S5. Steady-state PL of three HTLs on FTO/Glass substrate

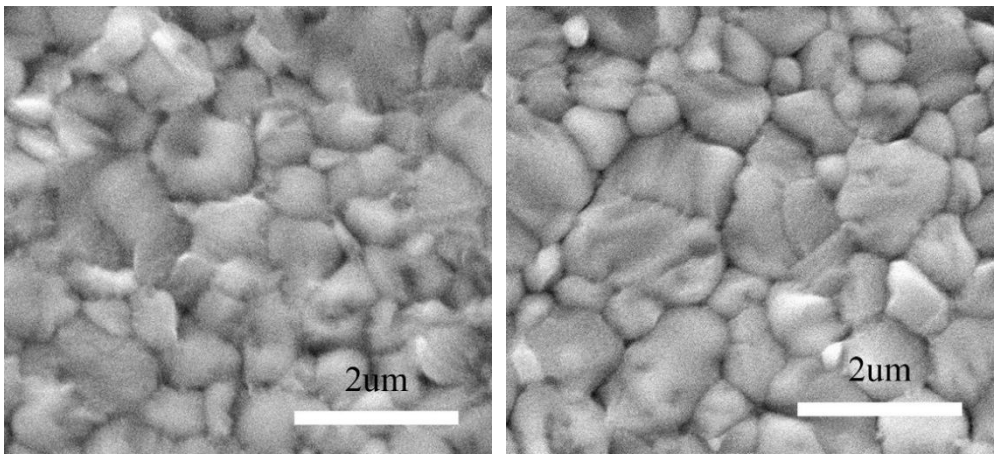

(a) (b)

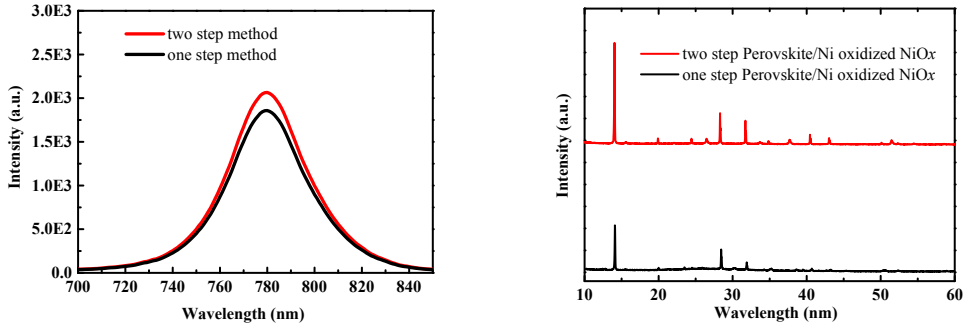

(c) (d)

Fig. S6. (a)SEM of one step solution method perovskite layer (b) SEM of two step solution method perovskite layer (c)PL of two methods prepared perovskite layer (d) XRD of two methods prepared perovskite layer

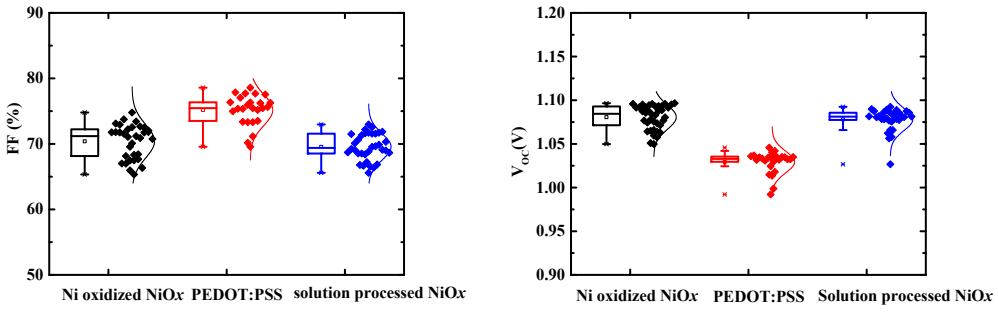

(a) (b)

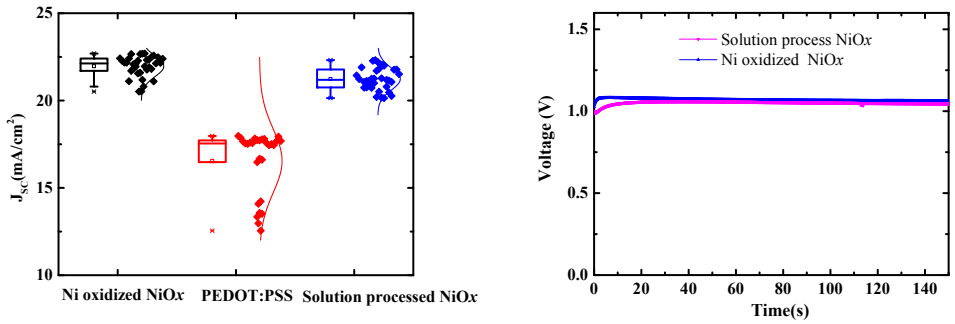

(c) (d)

Fig. S7. Comparison of histograms of photovoltaic parameters V_{OC} for the PSCs based on the two step process method. (a) Comparison of FF for the PSCs. (b) Comparison of Voc for the PSCs, (a) Comparison of Jsc for the PSCs. Data from sixteen Cells were used for the histogram. Perovskite layers were formed by the two-step deposition method. (d) Steady-state measurements of V_{OC}

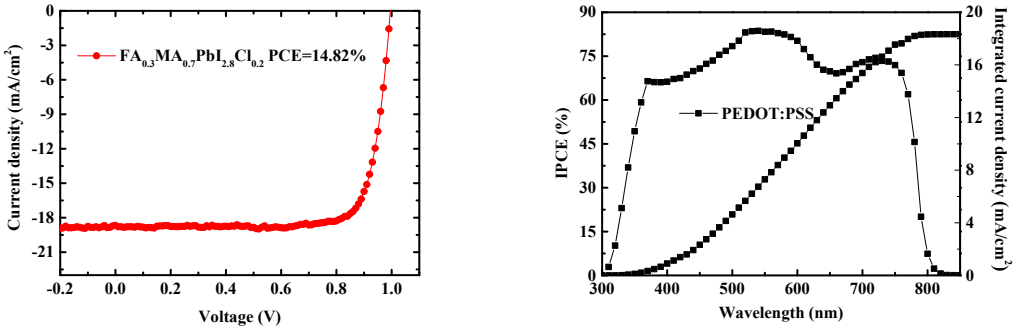

(a) (b)

Fig. S8. (a) The best *J–V* curve for device with PEDOT:PSS HTL. (b) The IPCE spectra and corresponding integral current for the best device based on PEDOT:PSS HTL

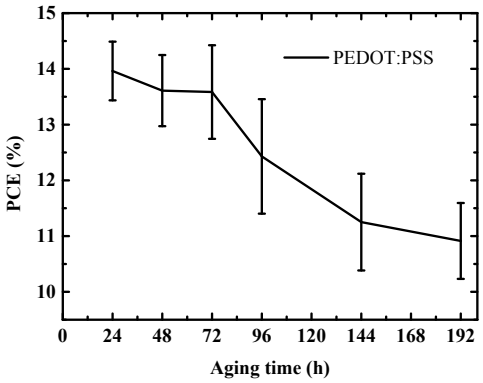

Fig. S9. The air stability of unencapsulated devices based on PEDOT:PSS HTL

Table S1. The comparison among different NiO_x based devices in this work and literatures.

Device Configuration	V_{oc} **(V)**	J_{sc} **(mA/cm^2)**	**FF**	**PCE (%)**	**Ref**
Glass/FTO/NiO(Ni oxidized NiO*x*)/$MA_{1-y}FA_yPbI_{3-x}Cl_x$/PCBM/BCP/Ag	1.09	22.2	0.74	17.8	This work
Glass/ITO/NiO/DEA/$CH_3NH_3PbI_3$/C_{60}(CH2)(Ind)/PN4N/Ag	1.13	20.4	0.80	18.1	[6]
Glass/ITO/NiO(NCs)/$CH_3NH_3PbI_3$/C_{60}/Bis-C_{60}/Ag	1.03	21.8	0.78	17.6	[7]
Glass/ITO/PLD-NiO/$CH_3NH_3PbI_3$/PCBM/LiF/Al	1.06	20.2	0.81	17.3	[8]
Glass/FTO/TiO_2/ $MA_{1-y}FA_yPbI_{3-x}Br_x$ /NiO-Spiro-MeOTAD/Ag	1.08	22.7	0.70	17.2	[9]
Glass/ITO/NiO(sf)/$CH_3NH_3PbI_3$/PCBM/Ag	1.04	21.2	0.75	16.6	[10]
Glass/ITO/NiO(ALD)/ $CH_3NH_3PbI_3$/PCBM/Ag	1.04	21.9	0.72	16.4	[11]
Glass/FTO/NiO(solution)// $CH_3NH_3PbI_3$/PCBM/Ag	0.99	20.5	0.78	15.7	[12]
Glass/ITO/NiO(ALD)/ $CH_3NH_3PbI_xCl_{3-x}$/PCBM/Ag	1.05	22.8	0.65	15.5	[13]
Glass/ITO/NiO(sputter)/ $CH_3NH_3PbI_xCl_{3-x}$/PCBM/AZO/Ag	1.08	20.33	0.69	15.2	[14]

References:

(1) Ghosh, D. S.; Betancur, R.; Chen, T. L.; Pruneri, V.; Martorell, J. Semi-Transparent Metal Electrode of CuNi as a Replacement of an ITO in Organic Photovoltaic Cells. *Sol. Energy Mater. Sol. Cells* **2011**.

(2) Liu, M.; Johnston, M. B.; Snaith, H. J. Efficient Planar Heterojunction Perovskite Solar Cells by Vapour Deposition. *Nature* **2013**, *501* (7467), 395–398.

(3) Jeong, S.; Woo, K.; Kim, D.; Lim, S.; Kim, J. S.; Shin, H.; Xia, Y.; Moon, J. Controlling the Thickness of the Surface Oxide Layer on Cu Nanoparticles for the Fabrication of Conductive Structures by Ink-Jet Printing. *Adv. Funct. Mater.* **2008**.

(4) Iijima, J.; Lim, J. W.; Hong, S. H.; Suzuki, S.; Mimura, K.; Isshiki, M. Native Oxidation of Ultra High Purity Cu Bulk and Thin Films. *Appl. Surf. Sci.* **2006**.

(5) Morita, M.; Ohmi, T.; Hasegawa, E.; Kawakami, M.; Ohwada, M. Growth of Native Oxide on a Silicon Surface. *J. Appl. Phys.* **1990**.

(6) Xue, Q.; Bai, Y.; Liu, M.; Xia, R.; Hu, Z.; Chen, Z.; Jiang, X. F.; Huang, F.; Yang, S.; Matsuo, Y.; Yip, H.; Cao, Y. Dual Interfacial Modifications Enable High Performance Semitransparent Perovskite Solar Cells with Large Open Circuit Voltage and Fill Factor. *Adv. Energy Mater.* **2017**, *7* (9), 1–9.

7) Zhang, H.; Cheng, J.; Lin, F.; He, H.; Mao, J.; Wong, K. S.; Jen, A. K. Y.; Choy, W. C. H. Pinhole-Free and Surface-Nanostructured Niox Film by Room-Temperature Solution Process for High-Performance Flexible Perovskite Solar Cells with Good Stability and Reproducibility. *ACS Nano* **2016**, *10* (1), 1503–1511.

(8) Park, J. H.; Seo, J.; Park, S.; Shin, S. S.; Kim, Y. C.; Jeon, N. J.; Shin, H. W.; Ahn, T. K.; Noh, J. H.; Yoon, S. C.;. Hwang C S.; Seok S. Efficient CH3NH3PbI3Perovskite Solar Cells Employing Nanostructured P-Type NiO Electrode Formed by a Pulsed Laser Deposition. *Adv. Mater.* **2015**.

(9) Cao, J.; Yu, H.; Zhou, S.; Qin, M.; Lau, T.-K.; Lu, X.; Zhao, N.; Wong, C.-P. Low-Temperature Solution-Processed NiO_x Films for Air-Stable Perovskite Solar Cells. *J. Mater. Chem. A* **2017**.

(10) Ciro, J.; Ramírez, D.; Mejía Escobar, M. A.; Montoya, J. F.; Mesa, S.; Betancur, R.; Jaramillo, F. Self-Functionalization behind a Solution-Processed NiOx Film Used As Hole Transporting Layer for Efficient Perovskite Solar Cells. *ACS Appl. Mater. Interfaces* **2017**, *9* (14), 12348–12354.

(11) Seo, S.; Park, I. J.; Kim, M.; Lee, S.; Bae, C.; Jung, H. S.; Park, N.-G.; Kim, J. Y.; Shin, H. An Ultra-Thin, Un-Doped NiO Hole Transporting Layer of Highly Efficient (16.4%) Organic–inorganic Hybrid Perovskite Solar Cells. *Nanoscale* **2016**, *8* (22), 11403–11412.

(12) Yin, X.; Yao, Z.; Luo, Q.; Dai, X.; Zhou, Y.; Zhang, Y.; Zhou, Y.; Luo, S.; Li, J.; Wang, N.; Lin H. High Efficiency Inverted Planar Perovskite Solar Cells with Solution-Processed NiO x Hole Contact. *ACS Appl. Mater. Interfaces* **2017**.

(13) Qiu, Z.; Gong, H.; Zheng, G.; Yuan, S.; Zhang, H.; Zhu, X.; Zhou, H.; Cao, B. Enhanced Physical Properties of Pulsed Laser Deposited NiO Films via Annealing and Lithium Doping for Improving Perovskite Solar Cell Efficiency. *J. Mater. Chem. C* **2017**, *5* (28), 7084–7094.

(14) Islam, M. B.; Yanagida, M.; Shirai, Y.; Nabetani, Y.; Miyano, K. NiOx Hole Transport Layer for Perovskite Solar Cells with Improved Stability and Reproducibility. *ACS Omega* **2017**.